Development of 400V Solar Array Technology for Low Earth Orbit Plasma Environment

Development of 400V Solar Array Technology for Low Earth Orbit Plasma Environment

Satoshi Hosoda, Teppei Okumura, Jeong-ho Kim, Kazuhiro Toyoda and Mengu Cho

Laboratory of Spacecraft Environment Interaction Engineering

Kyushu Institute of Technology

1-1, Sensui-cho, Tobaka-ku, Kitakyushu, Fukuoka 804-8550 Japan

TEL / FAX: +81-93-884-3229

E-mail: hosoda@ele.kyutech.ac.jp

ABSTRACT

To realize 400 volts operation in LEO, we must overcome problems of arcing caused by interaction between spacecraft and surrounding LEO plasma. This paper is a summary report of laboratory tests carried out to develop 400V solar array technology. Among various designs tested, a design of covering solar array surface with transparent film, called film coupon, was the most promising mitigation method to prevent arc inception. We carried out various tests on the film coupons considering realistic situation encountered in orbit. The coupon biased to -400V in LEO-like plasma had no arc for more than 25 hours. Other tests involved UV exposure, AO exposure, thermal cycling and debris impact. Conductive substrate made of CFRP suffered many arcs at –400V. Sustained arc between a solar cell and the substrate was also observed upon simulated debris impact. Therefore, use of flexible substrate is adequate for 400V solar array in

LEO environment. To avoid the snapover effect near the positive end of array circuit, only negative part of the array circuit exceeding the arc inception threshold should be covered by film or an electron collector should be deployed.

1. Introduction

Use of high power in future space missions calls for high voltage power generation and transmission to minimize the energy loss during power transmission and the cable mass. In order to promote industrial use of Low Earth Orbit (LEO), such as manufacturing, sightseeing, or power generation, the power of a large LEO platform after the International Space Station (ISS) will soon reach the level of MW. High voltage power generation and delivery is a key technology to realize large LEO platforms.

We consider a simple circuit made of a power supply, *e.g.* solar array, generating power *P,* cable with total resistance of *R* and a load. Suppose that the transmission voltage is *V* and the power is delivered to the load with a current *I*, therefore $P=VI$, the power lost to the transmission cable, ΔP, is given by

$$\Delta P = RI^2 = P^2 \frac{R}{V^2} = P^2 \frac{\rho l}{SV^2}, \qquad (1)$$

where ρ is electric resistively of cables [Ω*m], l is cable length [m] and S : cross section of cables [m^2] . Therefore, a fraction of the total power lost to the cable is

$$\frac{\Delta P}{P} = P \frac{\rho l}{SV^2} \qquad (2)$$

This equation tells us that the larger the power the bigger loss to the cable. Unless we do something, sooner or later the power loss fraction exceeds unity as the power increases. In order to suppress the power loss fraction, there are four methods derived from Eq. 2: (i) Decreasing the cable resistance, (ii) Increasing the cross section of cables, (iii) Reducing the cable length and (iv) Increasing the transmission voltage. The method (i) is not technically feasible as super-conducting cable usable at orbital temperatures is not yet available. The method (ii) is not recommended as the cable mass increases. The method (iii) is effective, though we cannot expect remarkable reduction of the cable length without drastic change of solar array paddle and paddle boom structure. After all, the method (iv) is the most effective as the power loss is inversely proportional to the square of the voltage.

The rule of thumb is that as the power increases by two orders of magnitude the transmission voltage should increase by one order of magnitude. Generally speaking, the power generation voltage does not have to be the same as the transmission voltage. If we consider additional weight and loss associated with the use of DC-DC converters, however, the best solution is to generate the power at a high voltage as well. Currently, ISS, the largest spacecraft today, generates its power, approximately 100kW, at 160V and delivers it at 120V. If we were to use the next-generation high voltage solar array technology for 1MW-class spacecraft and extrapolate the relationship between the voltage and the power of ISS, we would require a solar array operating at 400V. As the post-ISS large space platforms will be most probably constructed in LEO, detrimental interactions between the spacecraft and the surrounding LEO plasma must be overcome [1]. The development of 400V solar array benefits not only a large space platform but also a satellite with a hall thruster, because the voltage is high enough to directly drive the

electric propulsion system without raising the voltage via a DC/DC converter [2].

Generally speaking, there are two ways to connect between the satellite body ground and solar array circuits. One is so-called “positive grounding “ in which the positive end of the solar array circuits are grounded to the satellite body. Another is so-called “negative grounding” in which the positive end of the solar array circuits are grounded to the satellite body. Although, there was serious examination carried out for the positive grounding of ISS [3], the negative grounding is by far the most common way of grounding. Therefore, we have developed the high voltage solar array technology implicitly assuming the negative grounding. In the present paper, we limit our discussion to the negative grounding case.

When a solar array generates electricity in LEO, the most of the voltage becomes negative with respect to the surrounding plasma potential due to mass difference between ions and electrons (Fig. 1). Ions charge insulator surface positively. Then the electric field near triple junction, where interconnector (conductor), adhesive (dielectric) and vacuum meet together is enhanced and an arc occurs [4]. There have been numerous studies on arcing on high voltage solar array in LEO condition. It is now known that an arc occurs once an array has a negative potential as low as -100V with respect to the ionospheric plasma [5,6]. An arc on solar array surface is usually a pulse of current whose energy is supplied by the electrostatic energy stored on the coverglass surface due to charging via positive ions. Such an arc is often called primary arc, trigger arc or primary ESD (electrostatic discharge).

We show a schematic of primary arc inception mechanism proposed by Refs.4 and 7 in Fig.2. For the case of solar array, the conductor in the figure corresponds to interconnector, solar cell electrode or bus-bar and the insulator in the figure corresponds to coverglass, adhesive or polyimide sheet. The primary arc inception occurs in the following manner,

1. Insulator surface is positively charged. The arrow in Fig.2 shows direction of electric field and illustrates that the field is intensified at the triple junction as the insulator surface accumulates positive charges.

2. As the electric field is further intensified, electrons are emitted from the conductor surface due to field emission. The potential structure around the triple junction forms electric field where field-emitted electrons are attracted to the insulator surface. The electrons incident on the insulator surface emit secondary electrons that leave positive charges near the triple junction and enhance the electric field further. The field emission electron current increases exponentially due to the feed-back mechanism.

3. As the field emission current increases, so does the electron incident current on the insulator. Then neutral gas is desorbed from the insulator surface due to the electron bombardment and forms a thin layer of the neutral gas. Discharge occurs as the neutral gas is ionized.

4. As the discharge occurs, the positive charges on insulator surface flow toward the conductor surface forming the discharge current. Excessive heat melts the conductor surface and the discharge becomes very similar to vacuum arc where metallic vapor is the source of ionization along with the neutral gas desorbed from nearby surface.

5. As electrons escape toward the ambient space from the discharge plasma, the charge stored on the capacitance between the spacecraft body and the ambient space is quickly discharged.

Then, the spacecraft body potential rapidly increases to near zero.

6. The arc plasma neutralizes the positive charge on the insulator surface via expansion of surface flashover. The arc ends as the surface flashover stops transferring energy to maintain the arc plasma.

7. The spacecraft body potential becomes negative again as the body acquires negative charges from the ambient plasma.

8. The insulator surface reacquires positive charges from the ambient plasma. As the surface charging proceeds, the situation goes back to the first step and repeats the process again.

Repeated primary arcs lead to surface degradation and electromagnetic interference. Destruction of solar cell PN junction due to intense arc current is another concern. Moreover, a single arc may momentarily shorten the array circuit. Then the current flows for a much longer time than a primary arc, such an arc is called secondary arc. A secondary arc may lead to permanent short-circuit in the array circuit and the arc current keeps flowing until thermal breakdown of insulator layer occurs. Such an arc is called sustained arc and believed to be the cause of the failure of Tempo-2 [8].

The purpose of the present paper is to report on the results of laboratory experiments carried out to develop solar array capable of generating electricity at 400V in LEO plasma environment. In order to develop high voltage solar array technology for 400V bus voltage, the next 4 steps are necessary;

- Suppress primary arc inception.
- Suppress the detrimental effects caused by primary arcs, such as surface deterioration, electromagnetic interference, and cell destruction.
- Prevent the transition from a primary arc to secondary arc.
- Prevent the loss of solar array electrical output even if a sustained arc occurs.

In the present paper we report on the studies on the first item. We have carried out preliminary tests with solar array coupon panels biased negatively inside a vacuum chamber [9]. Based on the preliminary results, several types of array coupon panels with various mitigation designs have been fabricated by a solar array manufacturer. Figure 3 shows a picture of base coupon that was made with fabrication process for conventional 100V satellites. This coupon serves as a benchmark regarding how effectively each coupon panel suppresses arcing. The test coupon panels are biased to a negative potential inside the vacuum chamber and various data are taken, such as rate of arc, arc current, position of arc, and so on.

To derive a numerical target for suppressing arc inception, we consider the performance degradation due to repeated primary arcs. In Ref.10, we biased a base coupon in LEO-like plasma to -400V and found that silicon solar cells degraded with a probability of once every 150 primary arcs. Arcs on the edge of solar cell often damage solar cell PN junction and make P and N electrodes short-circuited. This degradation occurs only for individual cells where the primary arc occurred. If primary arcs accumulate and kill one cell after another, the total voltage of the solar array string may eventually become lower than the minimum voltage required by a power control unit. Then the spacecraft loses the power from the string. Assuming 30 years operation in orbit, the allowable number of arcing that limits the arc-induced power degradation below 1% is estimated as follows: The probability of electrical performance degradation is 0.7% (once every

150 primary arcs). Once an arc occurs, the arc plasma propagates and neutralizes the positive charge on the coverglass within 4 meters radius [11]. This area includes approximately 5000 cells for the cell size of 7*cm* x 3.5*cm*. Thus the permissible arc number under the condition of 1% degradation is about 7300 arcs (=5000 x 0.01 / 0.007). Assuming 30 years operation in LEO, total time of power generation is about 180 thousand hours. Therefore, we should suppress arcing at least as little as one in 25 hours (=180000/7300) at -400V.

To suppress arc inception, there are several ideas. Two important processes of arc inception mechanism are enhanced electric field at the triple junction and secondary electron emission from the dielectric material. Thus, coupons were designed along the following strategies;

(1) Shielding the triple junction from plasma

(2) Prevent the secondary electron emission avalanche

(3) Decrease the electric field at triple junction.

To shield the triple junctions, we used ETFE (Ethylene-Tetra Fluoro Ethylene copolymer) film and large plate of glass covering multiple cells. To prevent the secondary emission avalanche we used overhanging coverglass and coverglass with ditched side surface. To decrease the electric field, we used Indium Tin-Oxide (ITO) coated coverglass and thick coverglass. We fabricated coupons incorporating these ideas and examined an arc mitigation performance in LEO plasma environment. All the coupons raised the arc threshold voltage compared to conventional design.

Theoretical estimates on how effectively each method suppresses arc inception was carried out previously [12] and there is an analytical tool to estimate the frequency of repeated primary arcs for a given design of solar array [7]. Before resorting to the analytical method, we can easily guess from the theory described in Fig.2 that primary arc inception should be completely

suppressed if we can shield the triple junction. Indeed, the best performance of arc mitigation was obtained for the coupons shielding the triple junction from the plasma. By shielding the triple junction we can suppress the positive charging of insulator near the triple junction by ambient ions as the ions are physically blocked from reaching the insulator. The shield also prevents electrons from escaping the area near the triple junction. The electrons may be emitted via field emission or via secondary electron emission. As long as they are kept near the triple junction, the positive charging due to secondary electron avalanche cannot proceed.

There are several ways to shield the triple junction. One obvious way is to shield the exposed metallic parts by insulator coating. This method usually doesn't work, as the thin insulator coating is very likely to suffer cracks after thermal cycles in orbit. The use of large plate of coverglass covering multiple solar cells has several problems as it may break due to launch vibration or make very difficult to repair the underlying solar cells. The use of transparent film covering the solar array has several advantages over the other two methods, such as minimum additional weight, strength against thermal cycle, mechanical flexibility, easy access to the solar cells and so on. In the present paper, we report only the experimental results regarding the coupons with transparent film, film coupon, because this design showed the best performance in the preliminary tests and the most promising character, as we were to use on real spacecraft. The experimental results of the other designs are found in Refs. [9], [13]-[15].

In the second section of the present paper, we describe a laboratory test carried out to measure the arc suppression performance of the film coupons. In the third section, we describe laboratory tests to check whether the film coupon can withstand other environmental factors, such as UV, AO, debris impact and others. In the fourth section, we propose final design suitable for 400V

power generation in orbit. In the fifth section, we summarize the paper with suggestion of future works.

2. Suppression of arc inception

Figure 4 shows a schematic of experimental setup. The experiments of arc suppression characteristics were carried out with this setup. The vacuum chamber is 1*m* in length and 1.2*m* in diameter. The chamber can be pumped to a pressure as low as below $1x10^{-5}$ *Torr*. In order to simulate the LEO plasma environment, an ECR plasma source generated Xenon plasma.

We measured the plasma parameters by a Langmuir probe made by a disk of 30mm diameter. The plasma potential with respect to the chamber ground was *5 ~10 V*. When we refer to "bias voltage" in the present paper, it is the potential with respect to the chamber wall that served as the ground point of the experimental circuit. In the experiment, we biased solar array coupons to negative voltages. Strictly speaking the bias voltage should be referenced to the plasma potential. Because the bias voltage was more negative than -100V, the error is negligible and we used the chamber wall as the reference point rather than the chamber plasma potential that differs in each experiment. Typical electron density and electron temperature during the experiments were $2x10^{12}$ m^{-3} and *3 ~ 7 eV*, respectively. The electron density well simulated the highest value in the ISS orbit. Although, the electron temperature was over ten times higher than the value of the ISS orbit, it was still much lower than the coupon bias voltage. Because the coupons with a potential more negative than -100V attracts ions, the difference of electron temperature did not influence the time constant of surface charging via ions.

In Fig. 5, we show a schematic picture of external circuit connected to an array coupon. The strings are biased to a negative potential of 400V via a DC power supply through a limiting resistance of 100*kΩ*. To avoid arcing on CFRP back surface, we biased only the strings while the

coupon panel ground was grounded unless noted otherwise. In order to simulate the arc current supplied by coverglass on the solar array panel, we connect an external circuit [11]. The external circuit consists of a capacitance, inductance and resistance. We have attached a capacitance, $5\mu F$, and an inductance, $270\mu H$, and a resistance, 4Ω. The data recorded are the following; Arc position, arc current waveform, fluctuation of the background plasma condition and increase of background pressure. We developed an experimental system that can record all the arc events including waveforms and locations.

Figures 6, 7 and 8 show the film coupons that correspond to the first, second and third versions, respectively. These coupons use similar layout to the base coupon shown in Fig. 3. They have 7 x 3.5*cm* Si cell with IBF (integrated bypass function) on the aluminum honeycomb / CFRP substrate with Kapton® sheet. Four cells are connected in series and three strings are placed in parallel. For the first version, RTV Si was grouted between strings to prevent arcs at the gaps between cells with large potential difference. For the second and third versions, however, there was no grouting between strings, though bus bars were coated by RTV Si. These coupons have a transparent Teflon film covering over all the strings. The Teflon film made of ETFE whose thickness is $12.5\mu m$. It has a transmittance of about 95% between 400nm to 1μm wavelength. ETFE has the characteristic of radiation resistance. Because it was hard to adhere the film to substrate, the film was attached to adhesive supports at several points of film edges.

Figure 9 and 10 show the locations of arcs and the number of arcs for the base coupon. In this experiment, each bias voltage was applied for 90 minutes considering the orbital period in LEO. There are numerous arcs and the base coupon design is not adequate for 400V power generation in space. Figure 9 tells us that arc can occur anywhere around solar cells, especially on metallic electrodes such as interconnector or bus bars. As the voltage became higher, solar cell edges

began to arc and even edge covered with RTV Si arced at -500V. It is easy to cover bus-bars and solar cell edge with insulator such as RTV Silicon rubber to prevent arcs while avoiding problems associated with thermal cycling in orbit. Relying too much on insulator coating, however, may lead to weight increase and contamination. Also, arcs on interconnector are difficult to prevent by insulator coating as thermal cycle in orbit easily puts heavy mechanical stress and easily produces cracks on the insulator exposing the metallic surface.

Figures 11 and 12 show the number and locations of arcs observed for the first version of film coupon shown in Fig.6. Although the first version film coupon suppressed arcing well, it could not suppress arcing on the bus bars at high voltages. The reason of arcing on the bus bars was due to existence of the gap that was produced as the cables lifted the film from the Kapton® surface. Plasma entered from the small gap and charged dielectric material near the exposed bus bars. To reduce these gaps as small as possible, length between the cell edge and the film edge was doubled to give a buffer zone in the second version as shown in Fig.7. This buffer zone on the substrate gives little weight increase for flight solar panels because the buffer zone consists of a tiny portion of a large solar panel whose size is over 1m. In addition to the buffer zone, the bus bars of the second version were coated by RTV-Si rubber.

We biased the second version from -100V to -800V at every 100V for 90 minutes. The second version had no arcs up to -800V. Although, there were large potential deference between cell edge and plasma, ETFE film prevented the ambient ions from intruding to the triple-junction and the emitted electrons from escaping the triple-junction area to ambient plasma. Therefore, the enhancement of electron field near the triple-junction was suppressed.

We also carried out a long duration test where the second version coupon was biased to -400V for 28 hours. Considering the load for plasma source and vacuum pumps, the test was carried out

every 5hours with intermission of 2 hours. It was confirmed that the film coupon never suffered any arc for more than 28 hours at –400V. Therefore, the second version film coupon meets the specification of arc suppression described in the previous section, less than 1 arc per every 28 hours. The third version, that was made after we found problems at the thermal-cycle test of the second version coupon, was also tested for arc inception. There was no arc for 90minutes at -400V and -800V.

3. Realistic orbit environment tests

A. Debris and micrometeoroids impact

Micrometeoroids or space debris impact is a serious problem in LEO especially for a large space platform. In order to evaluate the strength against the hyper velocity particle impact, we carried out laboratory simulation of debris impact using the Two-Stage Light Gas Gun (TSLGG) of the Computational Mechanics Laboratory at Kyushu Institute of Technology. We carried out two shots. Each test projectile simulating a hyper velocity particle was made of polycarbonate with weight of 1.03 *gram* and 10mm in diameter. This size corresponds to the smallest size that cannot be defended by a bumper [16]. The projectile velocities were 3.4 *km/s* and 3.5 *km/s*. The coupon was placed in the vacuum chamber attached to the TSLGG.

Figure 13 shows the front side of the coupon after the two shots. The first projectile was aimed at the left center from the front to the back. This projectile hit the film support material directly, and the covered film around this support was broken off. But the other supports and film had little damage. The second projectile was aimed at the lower right form the back to the front. We were interested in seeing whether the broken pieces of substrate would fly in all the directions and cause extensive damage to the covered film. On the contrary there was almost no

damage except the area around the impact position. The film coupon has sufficient resistance against hyper velocity impact.

During the test with the first shot, an external circuit shown in Fig. 14 was connected to the coupon to examine a possibility of sustained arc induced by the dense plasma produced by debris impact. A flash of light was observed on the coupon. Figure 15 shows the arc current and inter-string voltage waveforms. The vertical axis of the top panel, arc current, is derived by subtracting the current measured at Cp2 from the current measured at Cp1. The horizontal axis corresponds to the elapsed time from the impact. About $500\mu s$ after the impact, the arc current began to flow and lasted until we manually turned off the power supply. After the experiment, the solar array string was short-circuited to the substrate with resistance of 40Ω. This result tells us that that string-substrate sustained arc may be induced by debris impact regardless whether debris hit the inter-cell region or not. It does not matter whether the solar array is covered by film or not. Therefore, from the viewpoint of sustained arc mitigation, we should use flexible substrate solar panel that has no conductive layer below solar cells.

One may question that holes produced by repeated particle impacts will make the film protection ineffective. As long as the holes are not directly over the metallic parts, primary arcs will not occur easily. We tested a film strip coupon shown in Fig. 16. The coupon had the film covers only over the interconnector exposing most area of coverglass. This coupon can be regarded as the appearance of the film coupon after many small holes are produced. We biased the coupon to a negative potential inside the plasma chamber and observed no arc in 90 minutes up to -400V. When a big hole penetrating beyond coverglass exposing the jagged triple junctions, as shown in Fig. 13 are opened, primary arcs are inevitable if the solar cell voltage exceeds the arc inception threshold. These exposed solar cells, however, are already damaged severely and

more primary arcs cause no more harm as long as secondary arcs are prevented.

The most important point regarding the debris impact is whether single debris destroys entire film and exposes many solar cells and associated triple junctions. The test result tells us that even a direct hit to the film fixation point exposes only a small number of solar cells. For small holes directly over triple junctions or big holes penetrating beyond coverglass, we have to accept the loss of individual cells associated with impact damage or repeated primary arcs and include the loss into the margin of the power budget during the spacecraft operational life by calculating the probability of appearance of those holes. The case where the exposed cell has a positive potential will be discussed later.

B. Thermal cycles in LEO environment

We checked the strength of the film against thermal cycles. The second-version film coupon experienced 164 cycles of -90 to +90℃, which corresponded to the temperature range at ISS orbit, in a chamber of atmospheric pressure. The maximum temperature of thermal cycle was much lower than the melting temperature of ETFE film (260℃.). Figure 17 shows the appearance of the coupon after thermal cycle test. Even though the film wrinkled, there was no degradation of electrical output. But, some cracks were observed at the film supports. The cracks were probably generated at the low temperature as the film shrank more than the substrate. The coefficient of contraction of the film is higher than that of substrate by one or two orders of magnitude. For this reason, excessive stress occurred at the film support. Based on this result, we modified the second version film coupon. We gave ample room of contraction to the film and moved the film supports to the backside as shown in Fig. 8. The third version film coupon passed

200 thermal cycles of -90 ~ +90℃. Also, we confirmed that no degradation of cell electrical output occurred even after the film wrinkled.

C. **UV irradiation and AO exposure**

In LEO environment, the film encounters serious UV irradiation and Atomic Oxygen (AO) erosion. Electrical power output may decrease as the film transmittance degrades. To evaluate the transmittance degradation due to UV and AO exposure, we carried out the acceleration tests of UV irradiation and UV-AO combined environment. We used a coupon shown in the right of Fig.18. This sample was made of aluminum plate substrate, Kapton sheet, silicon cell and ETFE film. We evaluated the transmittance degradation by measuring the electrical power output of the underlying silicon solar cell.

In case of UV irradiation test, we used a deuterium lamp attached to a vacuum chamber. The chamber pressure during the test was about 2×10^{-6} *Torr*. The UV intensity was 160 times AM0 when it was integrated between 120nm and 240nm and 530 times between 120nm and 160nm. Figure 19 shows the decrease of short circuit current (I_{sc}) measured for the silicon solar cell below the film. The short-circuit current decreased by 7% after exposure of 150 hours. Assuming the following conditions based on ISS orbit; (i) Orbit altitude: 400km, (ii) Orbit inclination: 51.6 degree, (iii) Daily hours of sunlight; 17 hour, the expose time of 150 hours corresponds to 4 ~ 13 years in orbit. From this result, ETFE film has sufficient durability against UV in this range of wavelengths.

Next we evaluated the transmittance change after combined exposure of AO and UV using a test facility at Tsukuba Space Center (JAXA). Two samples shown in Fig.18 were tested. One was with silicon cell under ETFE film and the other was with dual junction cell under the film.

The facility was equipped with 48 deuterium UV lamps and AO source using a repetitively pulsed CO_2 laser. The UV intensity was 5 times AM0 when it was integrated between 120nm and 160nm. Measured AO flux in this test was $1.7x10^{20}$ atoms/cm^2. Test was carried out during 30 hours. Assuming ISS orbit, AO flux of a year from October 2001 was $3.5x10^{21}$ atoms/cm^2 [17]. Therefore, the equivalent time of UV irradiation was 2 days and that of AO was 17 days.

We list the cell electrical outputs before and after the test in Table 1. Figure 20 shows the photograph before and after test. Although the film color turned white after the test, no transmittance degradation was confirmed. We compare the electron microscope photographs taken before and after the test in Fig. 21. Texture structure was formed on the film surface due to AO-induced erosion. Because these textures trapped and scattered incident light, the total transmitted intensity showed almost no change. Therefore, ETFE film keeps working as arc suppressor while maintaining good transparency even under exposure to UV and AO. One issue is how we slow down the erosion process by AO. Transparent coating resistant to AO or selection of other transparent film that is strong against AO and UV should be tried in future.

D. Arcing on the back surface of rigid substrate

All the coupons we tested so far use rigid substrate made of aluminum honeycomb and CFRP. The back surface is covered by CFRP that is partially conductive. When solar array is operated at 400V in LEO, the potential of the entire satellite conductive surface becomes –400V with respect to the plasma potential. The CFRP surface has many triple junctions because it consists of conductive carbon fiber and insulative resin. In the test to measure performance of arc suppression, the panel structure was not biased to avoid unnecessary arcs on CFRP surface. To study arcing on the back surface, we biased the entire panel to -400V in the plasma chamber. The second version film coupon was used for this test because no arc was likely to occur on the cell

side. Figure 22 shows the arc positions observed on the CFRP surface. There are two types of arc locations. One is at the CFRP surface and another is at the boundary between CFRP and Kapton® tape used to cover the frame edge. More than 400 arcs occurred in 5 minute. Because of this high arc frequency, the external capacitor was charged only to approximately -200V although the DC power supply was set to -400V. This result gives another reason to avoid a conventional rigid substrate for 400V solar array in addition to sustained arc upon debris impact.

4. Method of film arrangement on a solar array surface

The solar array surface during power generation collects ions and electrons from the surrounding plasma. Considering the vast area of solar array, it plays an important role to determine the satellite potential. In ordinary situation, the satellite potential in LEO plasma environment is negative comparable to the solar array output voltage because of the mobility difference between electrons and ions. If the entire surface of solar array was covered by film as shown in Fig. 23, however, only the satellite body collects ions and electrons. Therefore, the satellite potential will become equal to the ambient plasma potential. Therefore, the solar array under the film has positive potentials with respect to the plasma as high as the power generation voltage.

In LEO altitude, holes on the film due to debris impact are unavoidable and metallic parts with a positive potential will be exposed to the plasma. Then the exposed surface intensively collects electrons from the plasma, resulting in parasitic power loss to the plasma. At potentials greater than about +200V, large current collection so-called “snapover” would be induced from even a very small exposed area [18]. To solve this problem, we propose covering only a part of solar array by the film where a negative potential exceeds the arc inception threshold as shown in Fig.24. If

covering only a part of solar array is difficult, deploying an electron collector, a simple conductive plate is sufficient, connected to the positive end of the array as shown in Fig.25 can be another solution.

5. Conclusion

Basic development of solar array technology capable of generating power at 400V in LEO plasma environment has been completed now. Covering solar array surface with ETFE film is the most effective method that suppresses arc inception up to 800V. Even if it is used for 30 years in space, the damage caused by arcs can be kept below 1% of the total electrical output assuming the film is intact from other environmental factors. The strengths of the film design against, debris impact, thermal cycle, contamination, frictional charging, residual gas, UV exposure, and AO exposure were verified in the laboratory tests. Traditional rigid solar panel structure made of aluminum honeycomb and CFRP, however, is not suited for the high voltage operation. Short circuit due to sustained arc induced by debris impact and frequent arcs on partially conductive CFRP surface are the reasons. Flexible solar panel made of insulator substrate is suitable to avoid those problems. To avoid the snapover effect near the positive end of array circuit, the film should cover only a part exceeding the arc inception threshold or an electron collector should be deployed.

There are still several environmental factors to be looked at such as, improvement of resistance of film to UV, AO, quick ventilation of air below the film, frictional charging expected during launch, cumulative effects of pin-holes produced by small particles impact, fixation method to flexible paddle and others and durability against auroral electron charging.

To study the combined effect of the various environment factors, we will seek an opportunity

of flight experiment.

Acknowledgments

This study has been carried out as a part of Grants-in-Aid for Scientific Research by JSPS and Ground-based Research Announcement for Space Utilization promoted by Japan Space Forum. Also, authors thank Mitsubishi Electric Corporation for manufacturing all the coupons and testing thermal cycles. Also, authors thank the Computational Mechanics Laboratory of KIT for using TSLGG. Thanks also go to JAXA Institute of Space Technology and Aeronautics for carrying out the AO exposure test and analysis of the film samples.

References

[1] D. E. Hastings and H. Garrett, Spacecraft-Environment Interactions, Cambridge University Press, 2004, Cambridge

[2] G. A. Jongeward, I. Katz, M. R. Carruth, E. L. Raph, D. Q. King and T. Peterson, ”High Voltage Solar Arrays for a Direct Drive Hall Effect Propulsion System”, IEPC-01-327, *Proceedings of 27th International Electric Propulsion Conference*, Pasadena, October, 2001.

[3] D. C. Ferguson, D. B. Snyder and R. Carruth, “Findings of the Joint Workshop on Evaluation of Impacts of Space Station Freedom Ground Configurations”, NASA TM-103717, 1990.

[4] Hastings, D. E., Cho, M. and Kuninaka, H.: The Arcing Rate for a High Voltage Solar Array: Theory, Experiment and Predictions, J. Spacecraft and Rockets, 29, (1992), pp. 538-554.

[5] Vayner, B., Galofaro, J., Ferguson, D.: Interactions of High-Voltage Solar Arrays with Their Plasma Environment: Ground Tests, J. Spacecraft and Rockets, Vol. 41, No. 6, November, pp.1042-1050, 2004

[6] Davis, S., Stillwell, R., Andirario, W., Snyder, D., Katz, I.: EOS-AM Solar Array Arc Mitigation Design, SAE Technical Paper Series, 1999-01-2582, 34th Intersociety Energy Conversion Engineering Conference, Vancouver, Canada, August 1999.

[7] Hastings, D.E., Wyle, G. and Kaufman, D.: Threshold Voltage for Arcing on Negatively Biased Solar Arrays, J. Spacecraft and Rockets, 27, (1990), pp.539-544.

[8] I. Katz, V. A. Davis and D. B. Snyder, "Mechanism for Spacecraft Charging Initiated Destruction of Solar Arrays in GEO", AIAA98-1002, *36th Aerospace Sciences Meeting & Exhibit*, Reno, January, 1998.

[9] S. Hosoda, T. Okumura, K. Toyoda and M. Cho, "High Voltage Solar Array for 400V Operation in LEO Plasma Environment", *Proceedings of 8th Spacecraft Charging Technology Conference*, Huntsville, October, 2003.

[10] K. Toyoda, T. Okumura, S. Hosoda and M. Cho, "Degradation of High Voltage Solar Array Due To Arcing in LEO Plasma Environment", *Journal of Spacecraft and Rockets*, Vol. 42, No. 5, 2005, pp. 947-953.

[11] M. Cho, R. Ramasamy, M. Hikita, K. Tanaka and S. Sasaki, "Plasma Response to Arcing in Ionospheric Plasma Environment: Laboratory Experiment", *Journal of Spacecraft and Rockets*, Vol. 35, No.1, 2002, pp. 392-399.

[12] Mong, Renee and Hastings, Daniel E.: Arc mitigation on high voltage solar arrays J. Spacecraft and Rocket, 31, (1994), pp. 684-690.

[13] M. Cho, K. Shiraishi, K. Toyoda and M. Hikita, "Laboratory Experiment on Mitigation against Arcing on Solar Array in Simulated LEO Plasma Environment", AIAA2002-0629, *40th Aerospace Science Meeting*, January, 2002.

[14] S. Hosoda, T. Okumura, K. Toyoda and M. Cho, “Development of High Voltage Solar Array in LEO Plasma Environment”, *24th International Symposium on Space Technology and Science*, Miyazaki, Japan, June, 2004.

[15] T. Okumura, D. Qu, J. Kim, S. Hosoda, M. Cho, K. Toyoda and M. Ohkubo, “Experimental development of high voltage solar array in LEO plasma environment”, *Proceedings of 48th Space Sciences and Technology Conference*, Fukui, Japan, November, 2004. (in Japanese)

[16] “Protecting the Space Station from Meteoroids and Orbital Debris”, *National Academy Press*, Washington D.C., 1997.

[17] http://sees.tksc.nasda.go.jp/

[18] G. B. Hillard and D. C. Ferguson, “Solar array module plasma interactions experiment (SAMPIE): science and technology objectives”, *Journal of Spacecraft and Rockets*, Vol. 30, No. 4, 1993, pp.488-494.

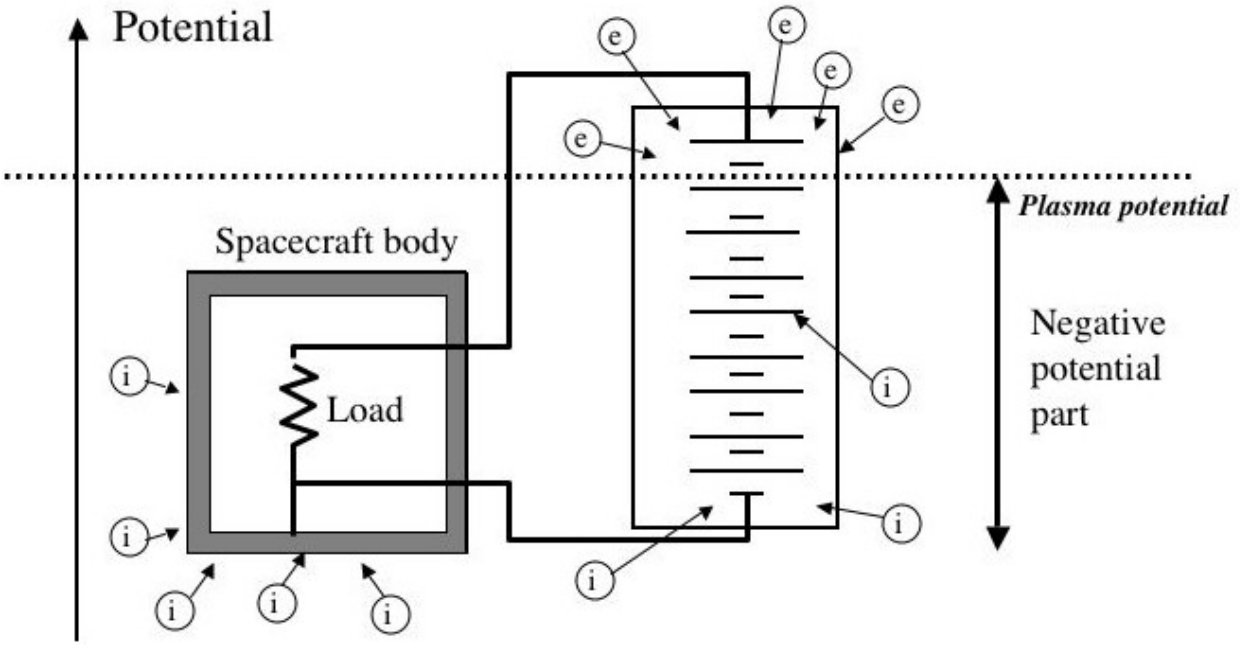

Figure 1: Schematic picture of satellite and solar array potential in case of negative grounding spacecraft

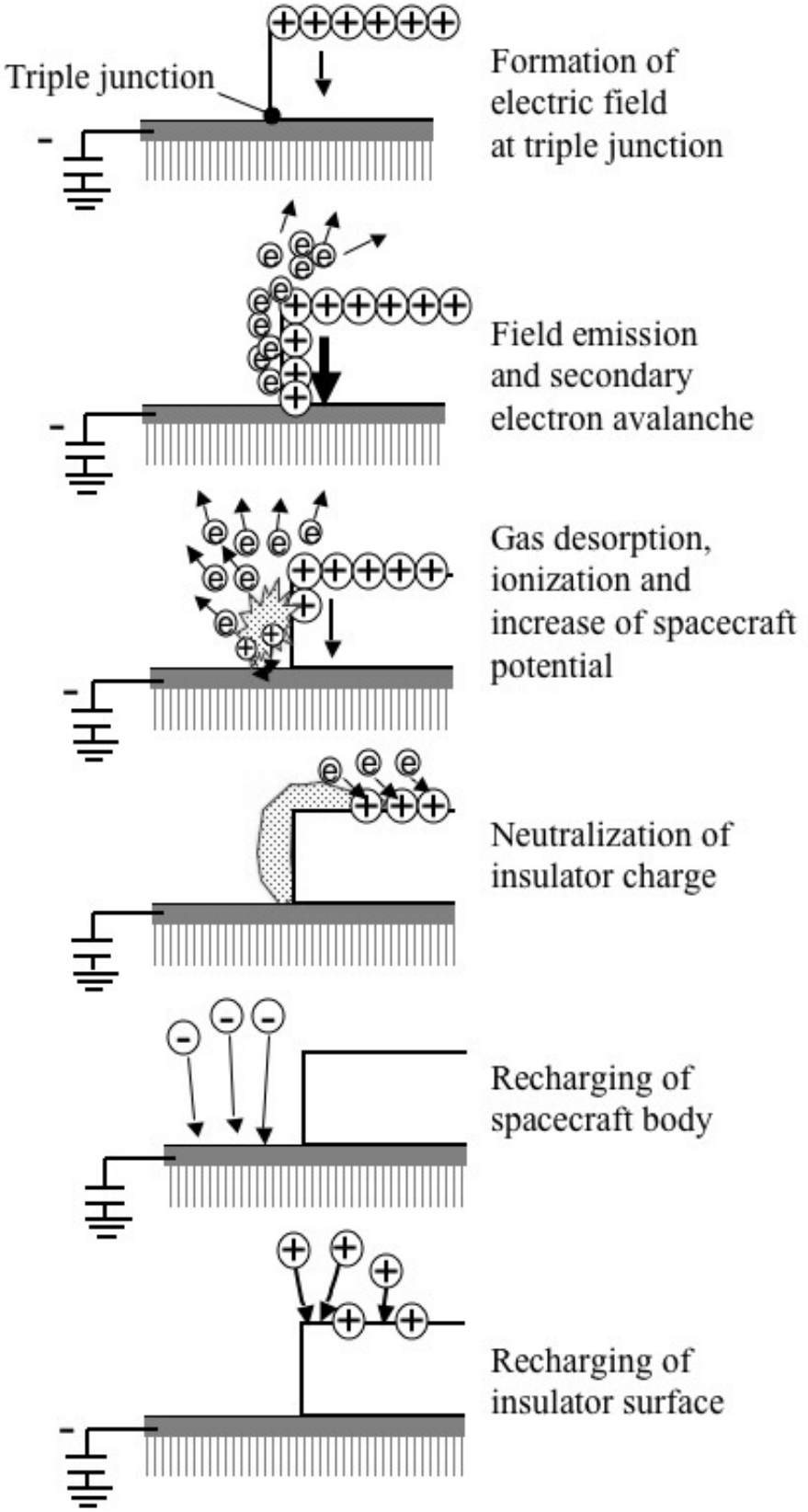

Figure 2: Schematic picture of primary arc inception at triple junction

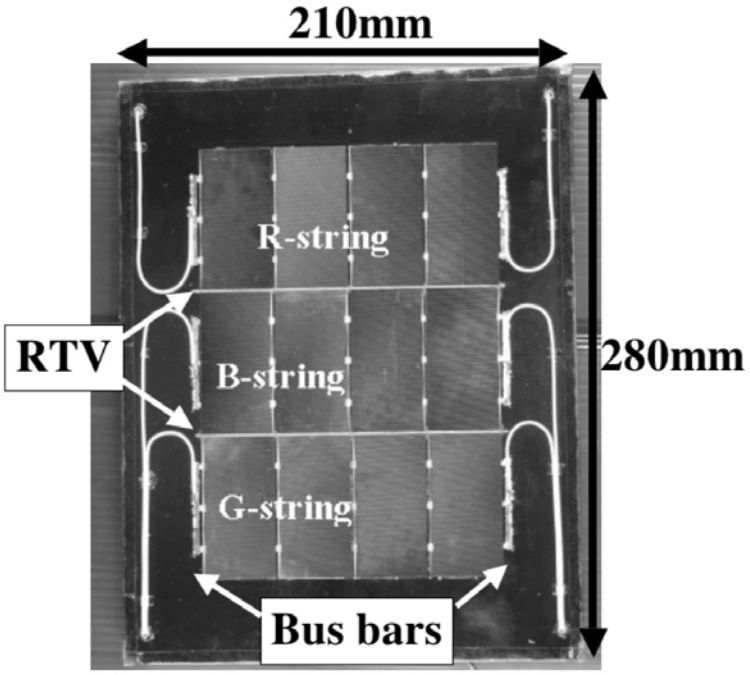

Figure 3: Photograph of base coupon that was made with conventional 100V satellites design

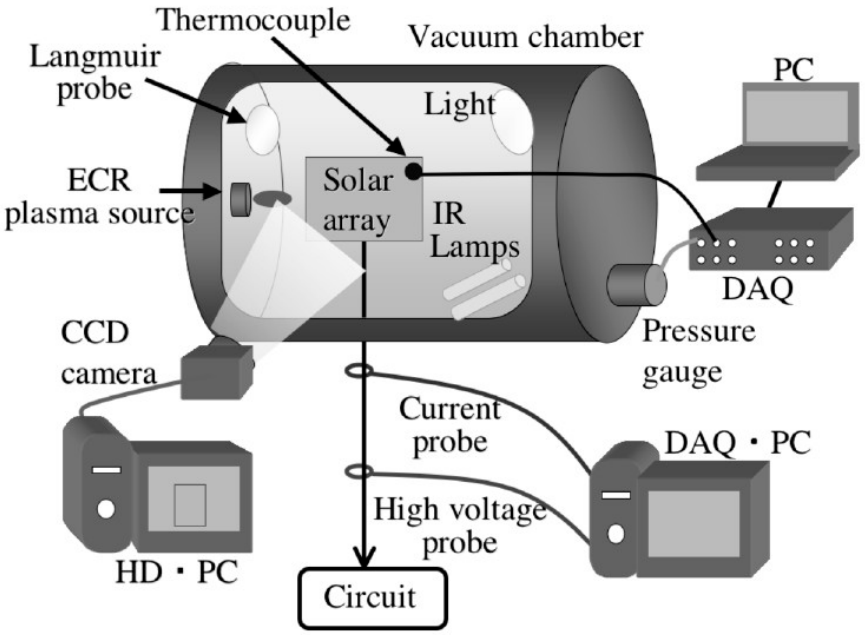

Figure 4: Experimental set-up for measurement of arc suppression characteristics

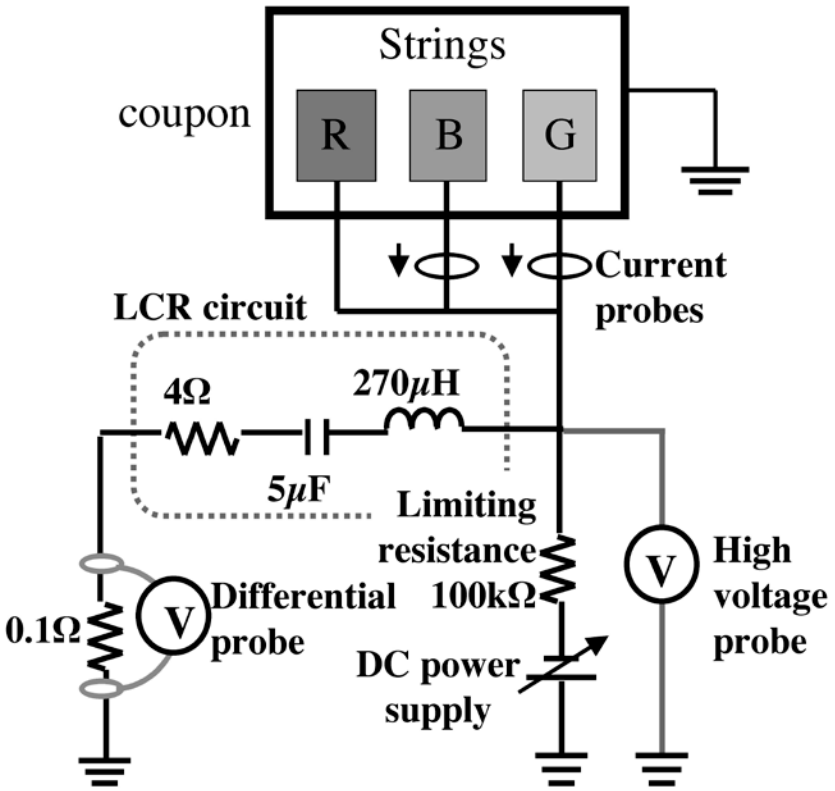

Figure 5: External circuit used for measurement of arc suppression characteristics at a bias voltage below –400V

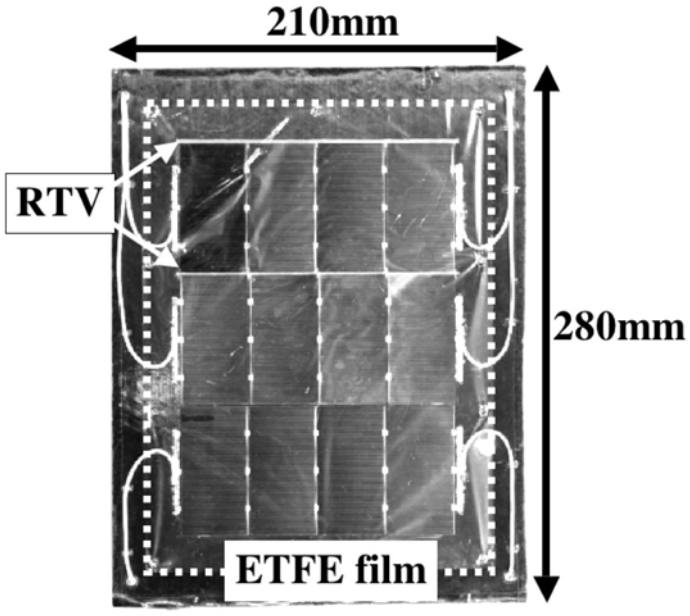

Figure 6: Photograph of the first version of film coupon

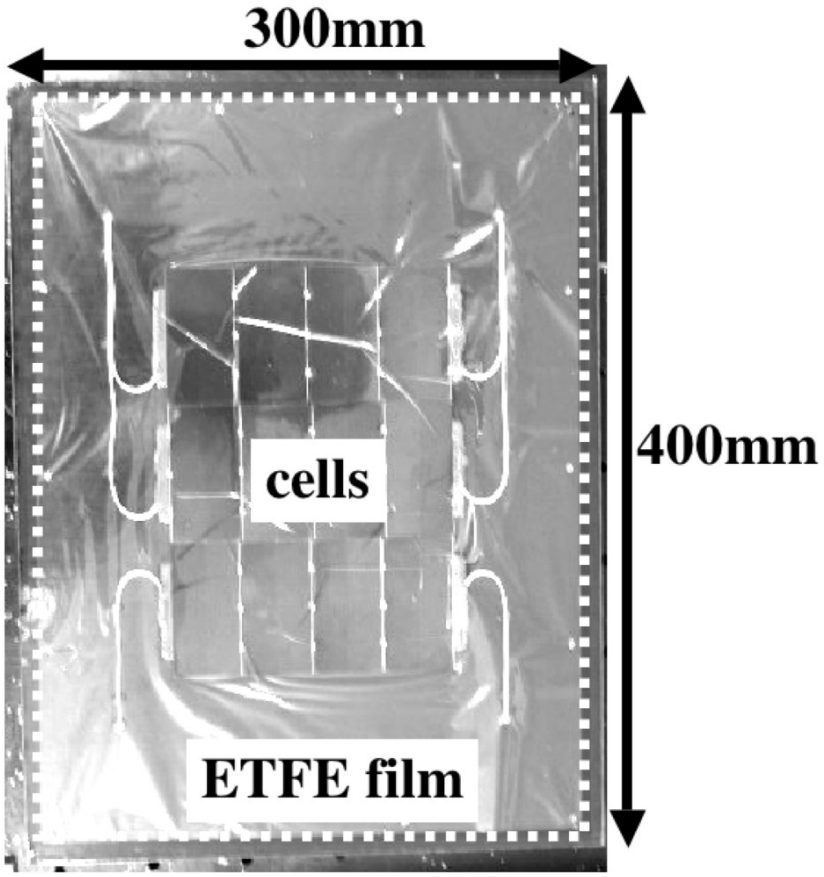

Figure 7: Photograph of the second version of film coupon. The distance between the cell edge and the ETFE film edge was doubled to give a buffer zone.

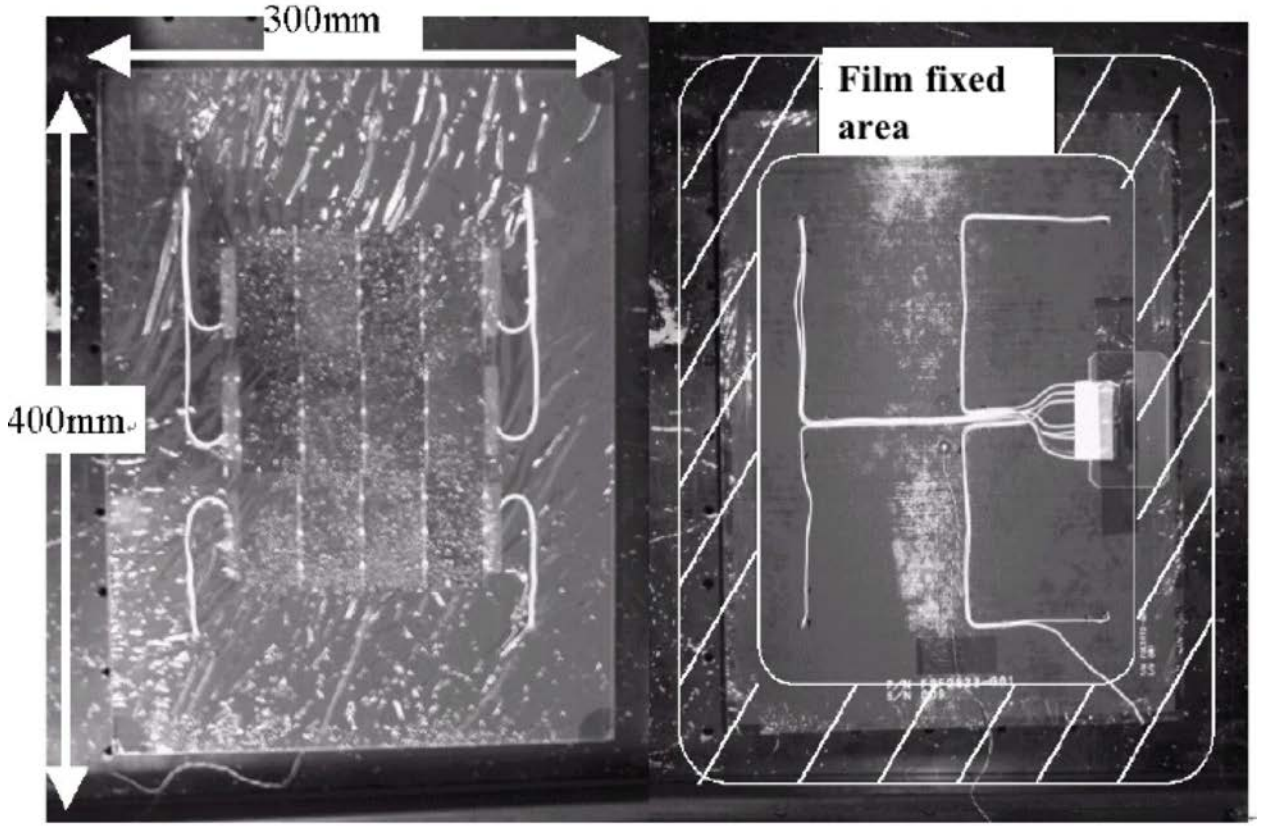

Figure 8: Photograph of the third version of film coupon. Front side (left) and back side (right). ETFE film covered almost all the front surface, and it was fixed on the back side.

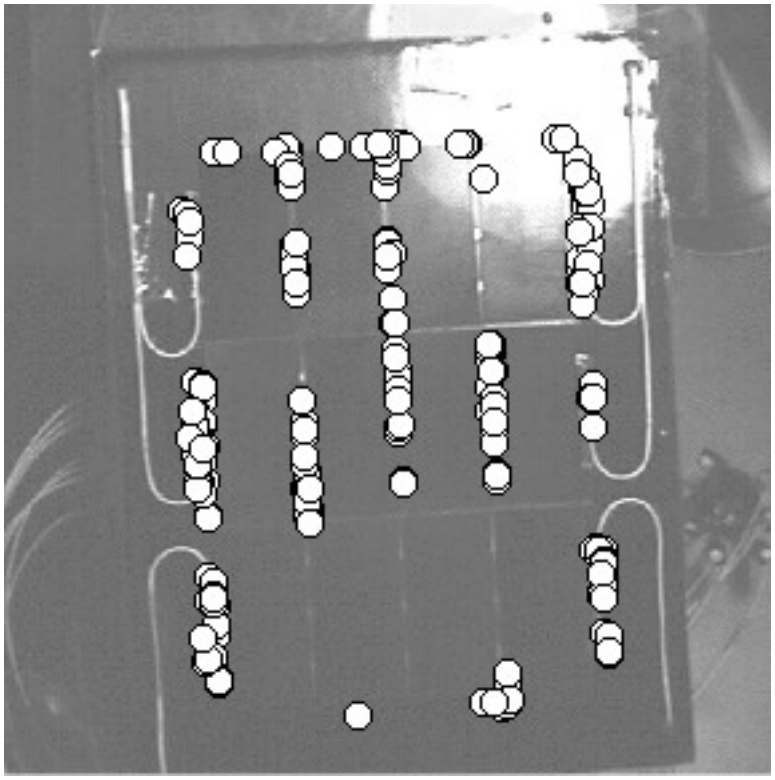

Figure 9: Locations of arcs observed on the base coupon

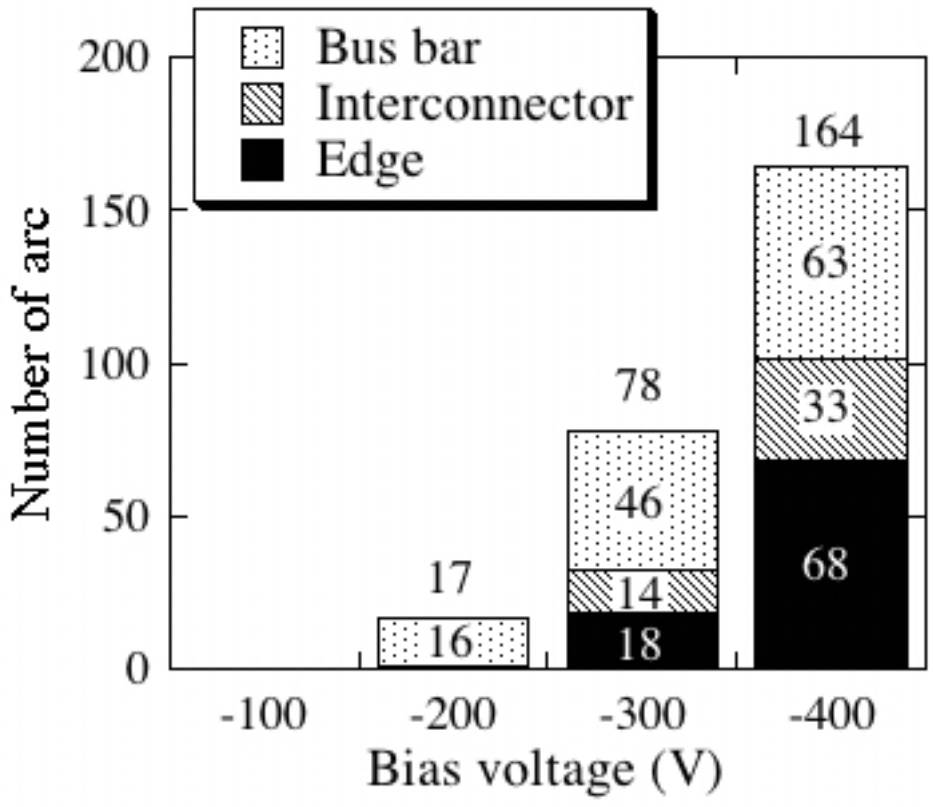

Figure 10: Number of arcs on the base coupon during 90minutes for each bias voltage

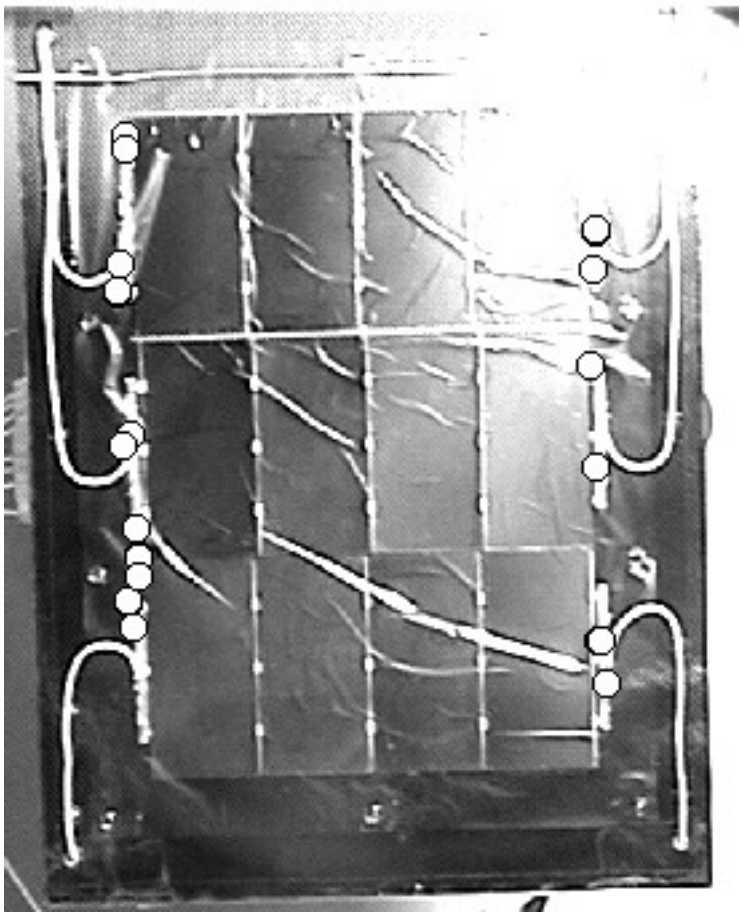

Figure 11: Locations of arcs observed on the first version of film coupon

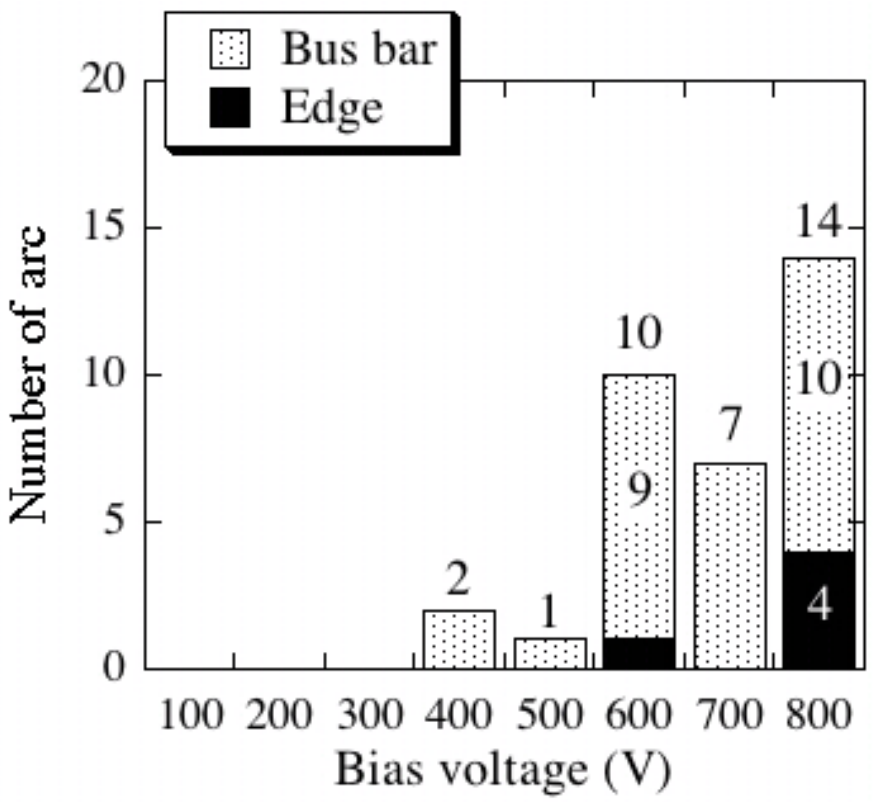

Figure 12: Number of arcs on the first version of film coupon during 90minutes for each bias voltage

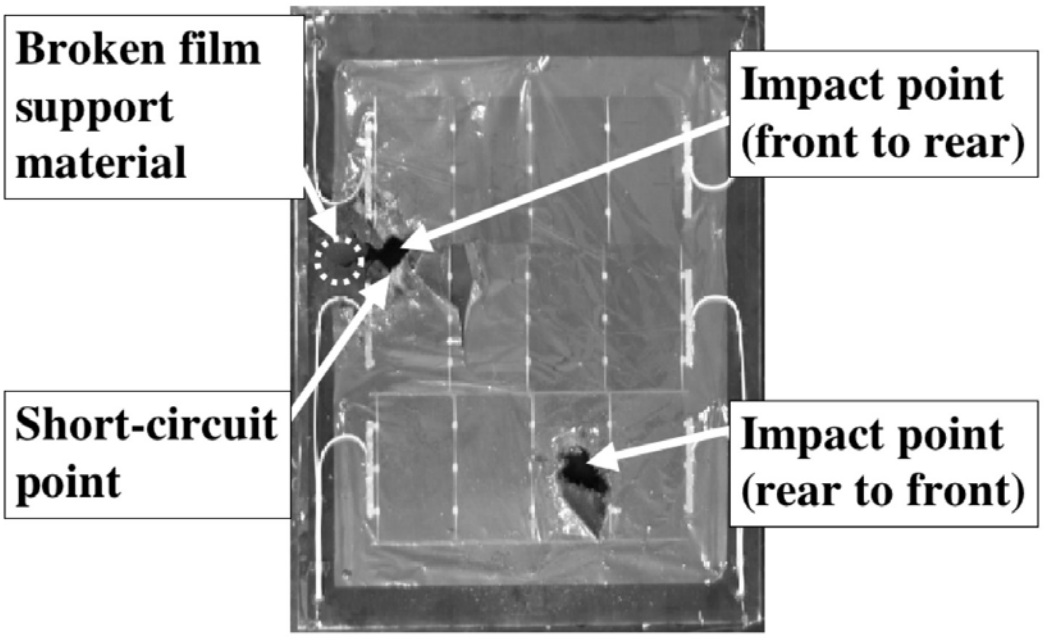

Figure 13: Photograph of the first version of film coupon after debris impacts

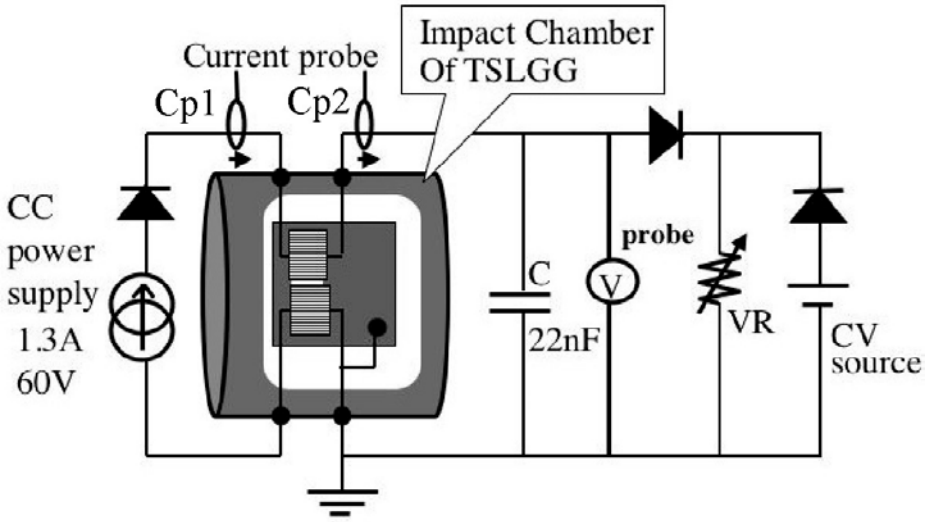

Figure 14: Experimental set-up to verify sustained arc phenomena under hyper velocity impact

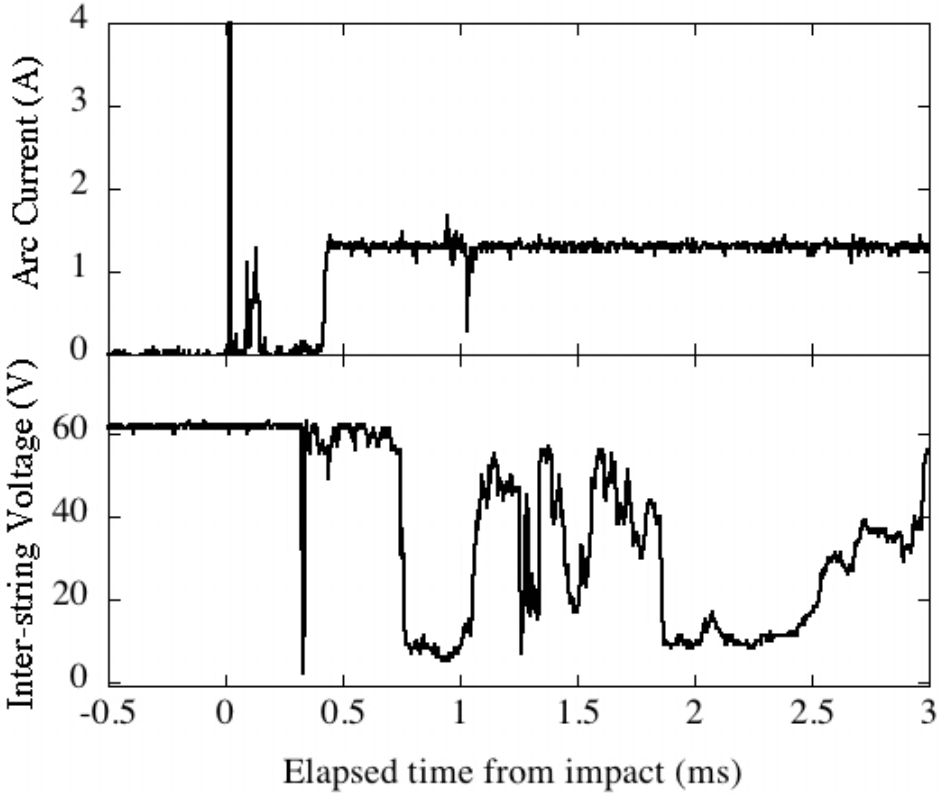

Figure 15: Measured waveform of sustained arc induced by simulated debris impact. Arc current (top) and inter-string voltage (bottom)

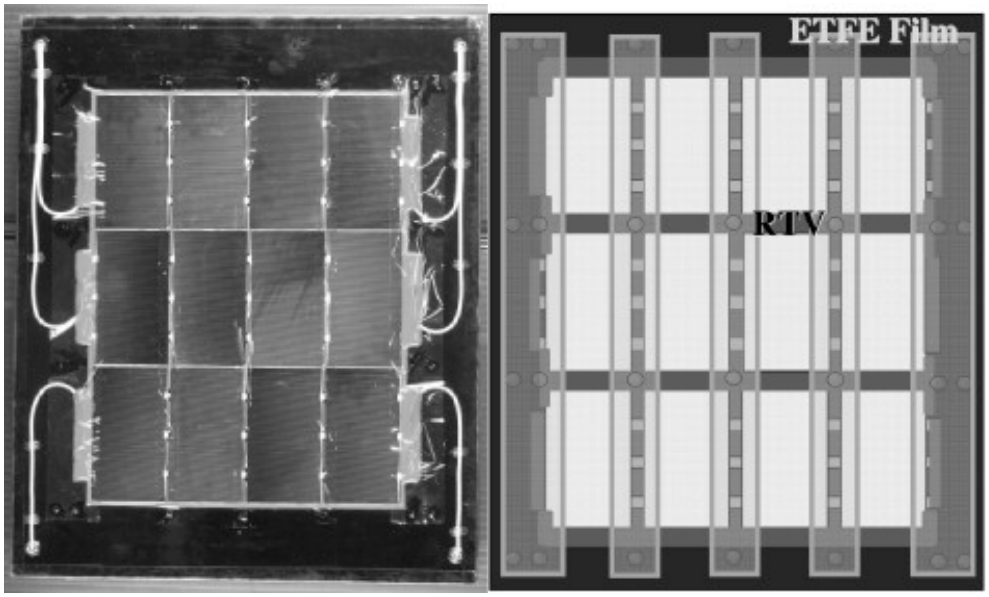

Figure 16: Photograph of film strip coupon (left) and its schematic picture (right)

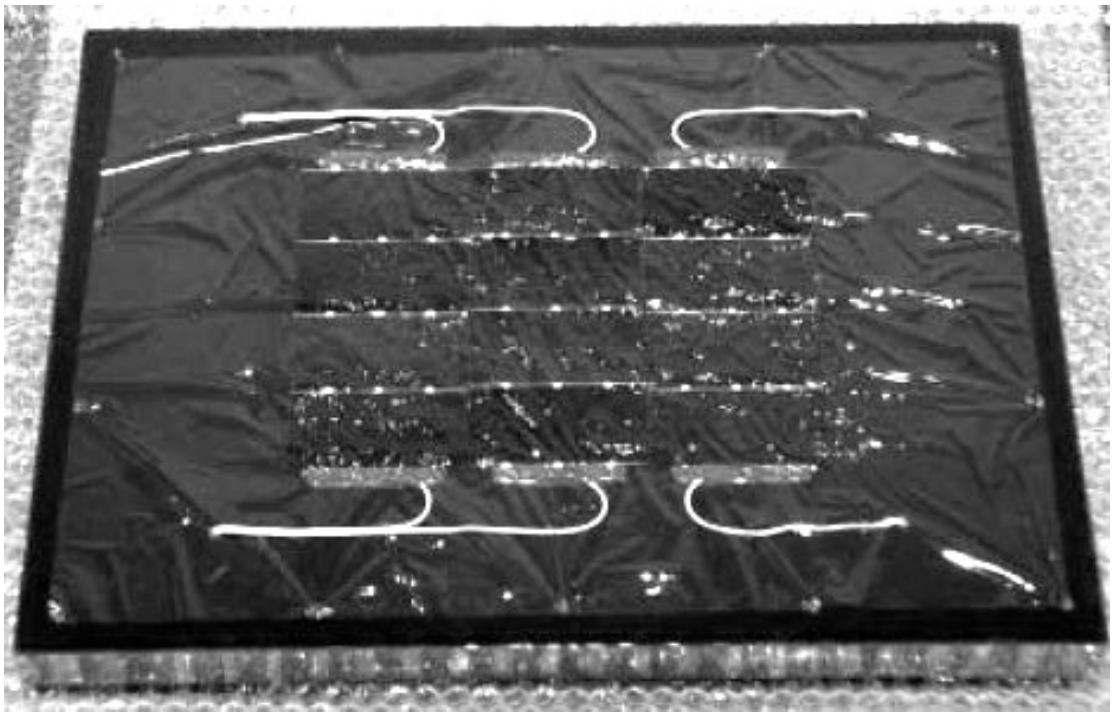

Figure 17: Photograph of second version film coupon after 164 thermal cycles

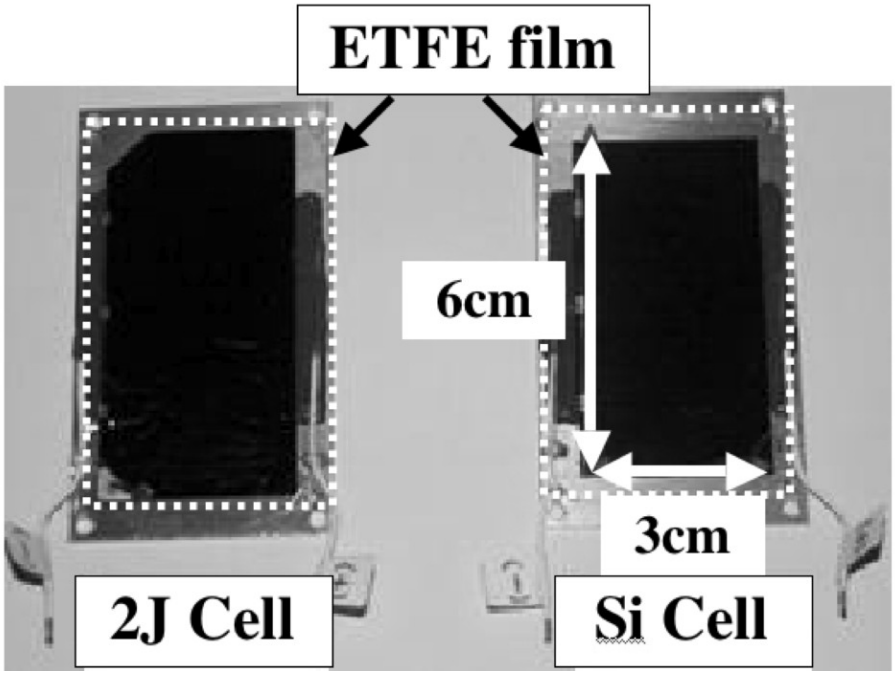

Figure 18: Photograph of film coupons for UV and AO exposure tests

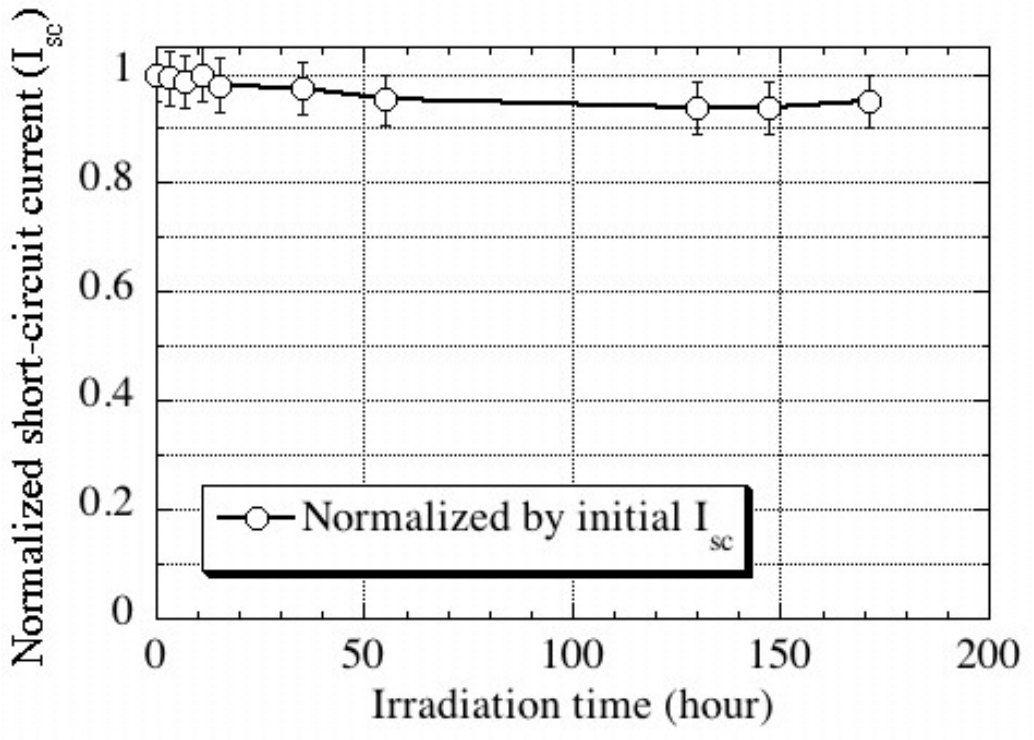

Figure 19: Decrease of short circuit current (I_{sc}) measured for the Si solar cell below the ETFE film exposed to UV radiation.

Table 1: Cell electrical outputs before and after AO exposure test.

		V_{oc} (mV)	I_{sc} (mA)	FF
Si cell sample	Before	610.6	1029.5	0.72
	After	610.9	1034.4	0.718
2J cell sample	Before	2346.3	404.3	0.863
	After	2348.1	406.6	0.868

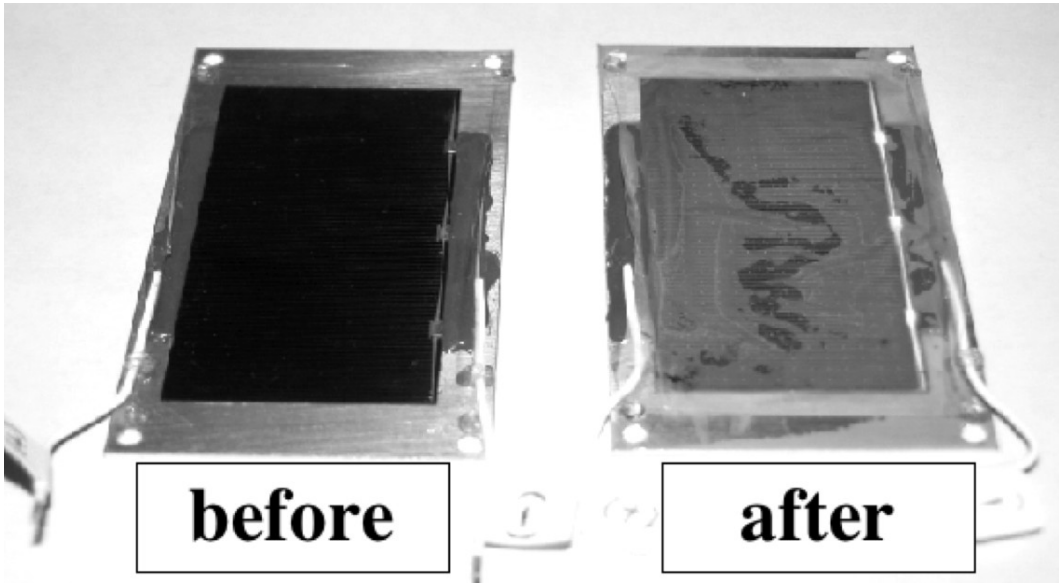

Figure 20: Photographs of film coupons before (left) and after (right) exposure to AO and UV combined exposure.

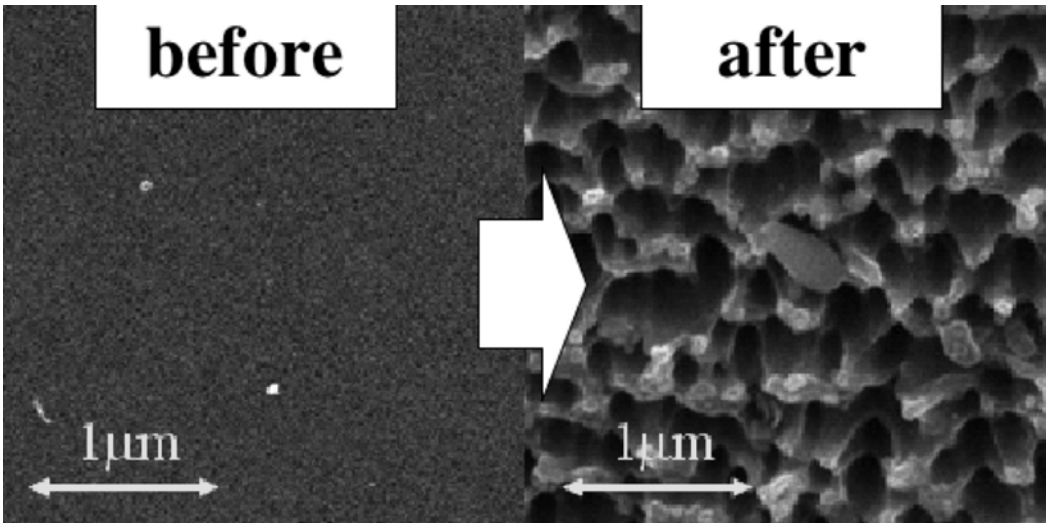

Figure 21: Microscope pictures of film surface before and after AO and UV exposure.

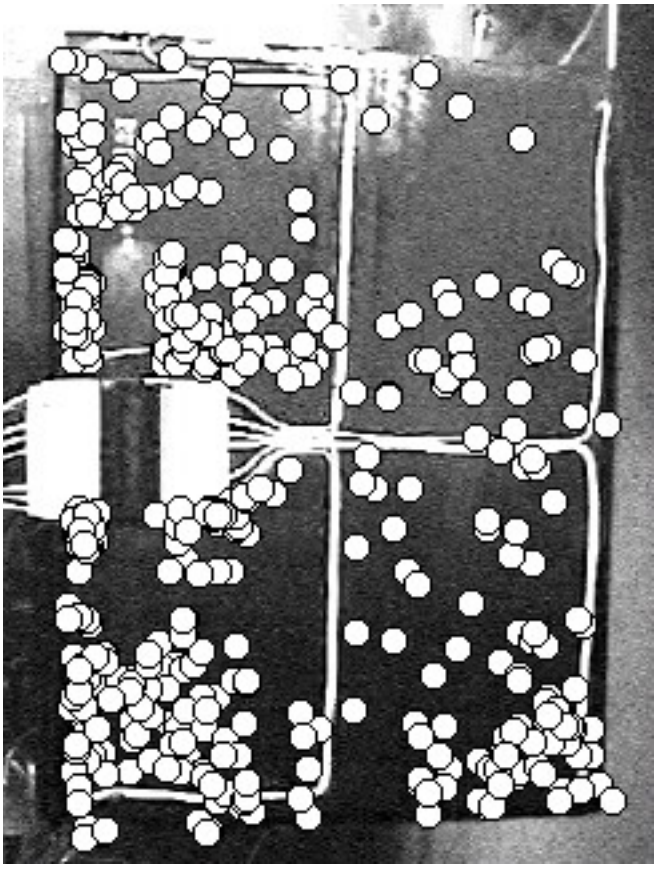

Figure 22: Arc positions on CFRP surface.

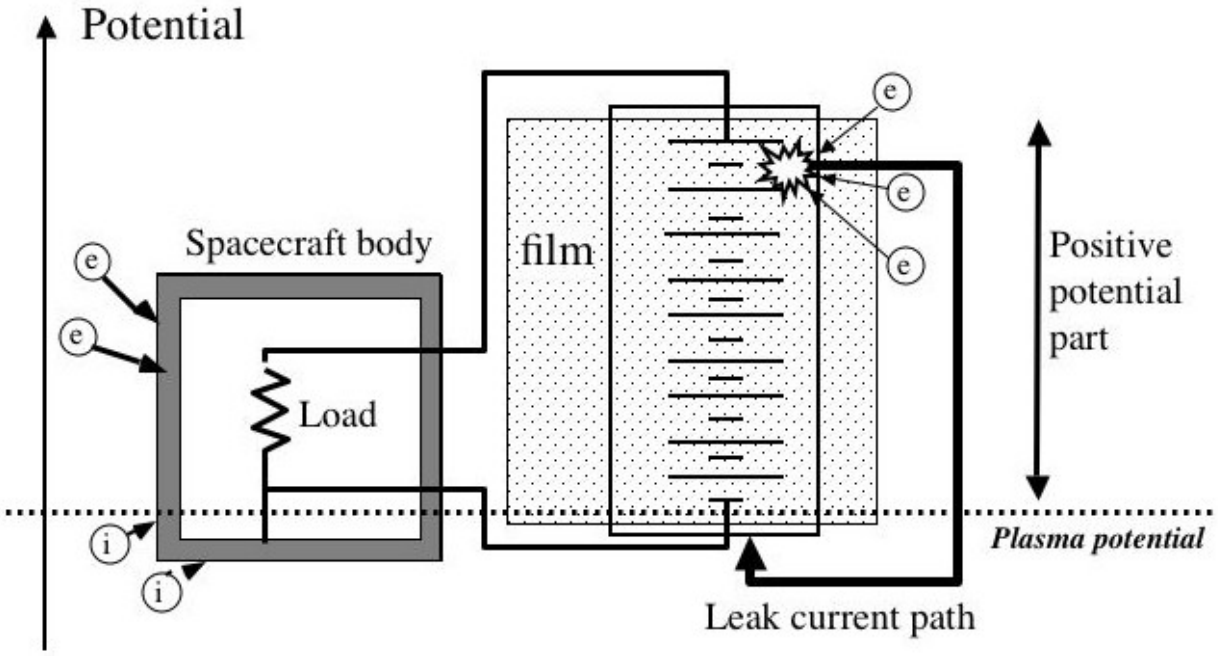

Figure 23: Satellite and solar array potential when entire array surface is covered by film.

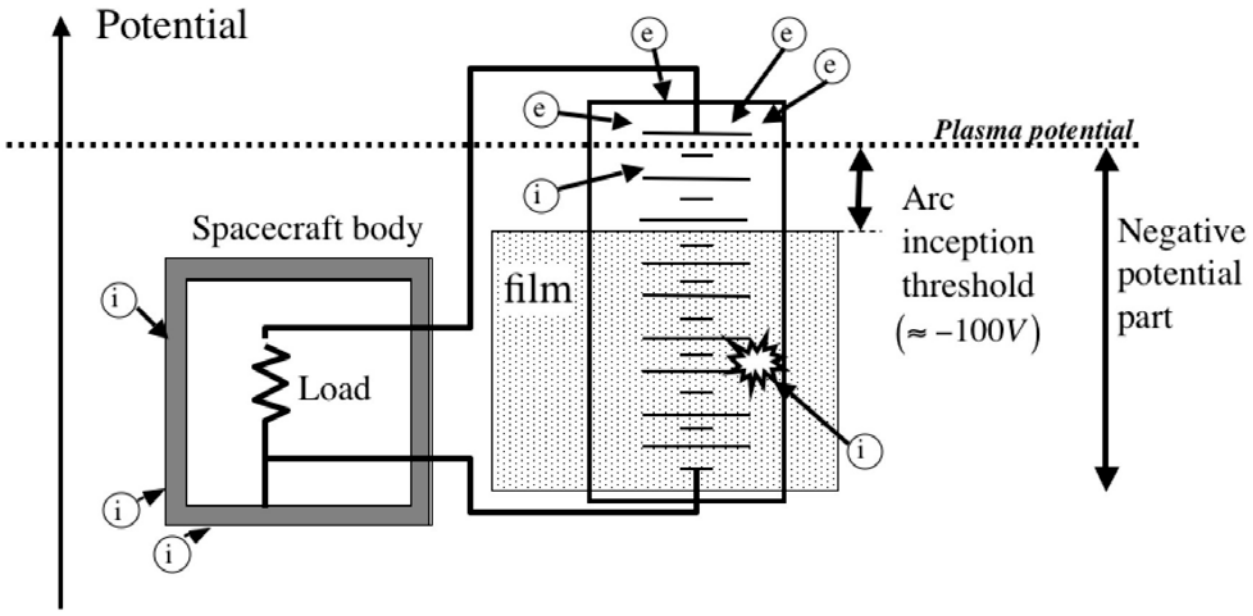

Figure 24: Satellite and solar array potential when a positive part of the array circuit is exposed to plasma.

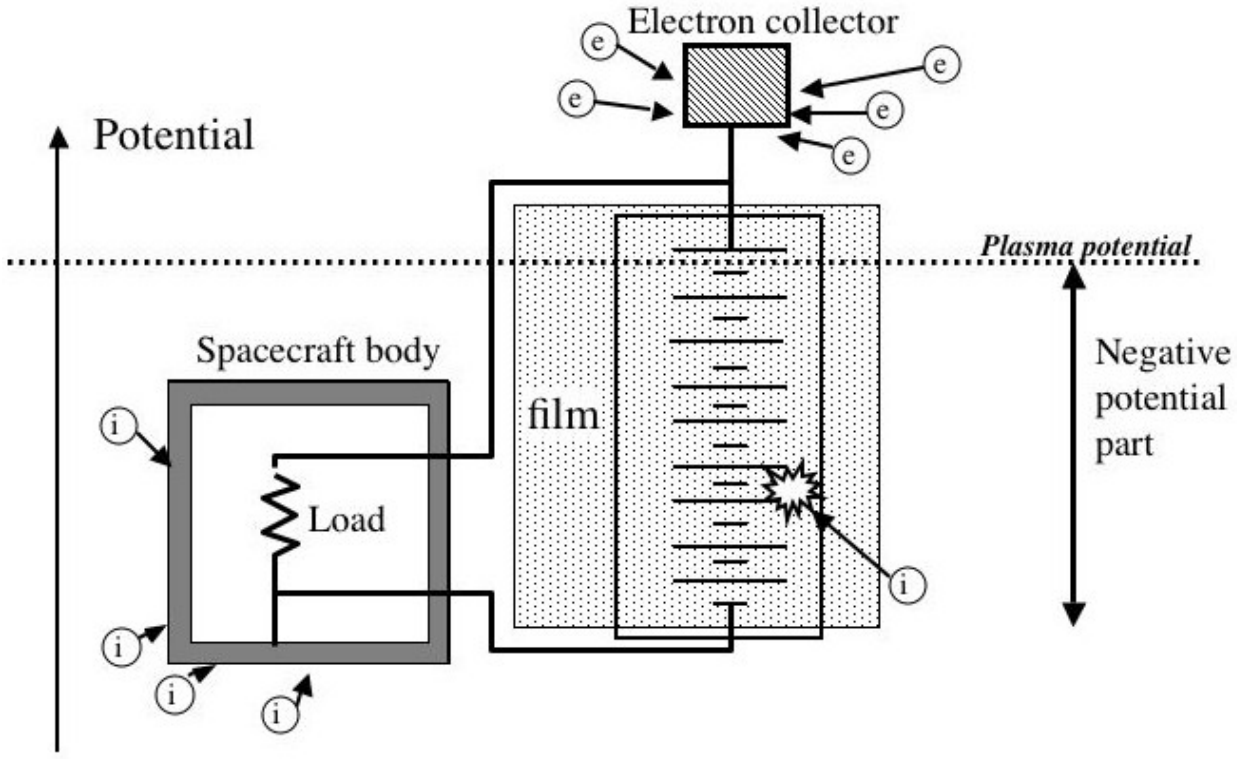

Figure 25: Satellite and solar array potential when an electron collector was connected to positive end.